PERGAMON

International Journal of Mechanical Sciences 43 (2001) 701–713

International Journal of MECHANICAL SCIENCES

www.elsevier.com/locate/ijmecsci

Size effects in ductile cellular solids. Part II: experimental results

E.W. Andrews[a], G. Gioux[a], P. Onck[b], L.J. Gibson[a,*]

[a]*Department of Materials Science and Engineering, Massachusetts Institute of Technology, 77 Massachusetts Avenue, Cambridge, MA 02139, USA*

[b]*Micromechanics of Materials, Delft University of Technology, Delft, The Netherlands*

Received 20 September 1999; received in revised form 12 May 2000; accepted 15 May 2000

Abstract

There is increasing interest in the use of metallic foams in a variety of applications, including lightweight structural sandwich panels and energy absorption devices. In such applications, the mechanical response of the foams is of critical importance. In this study, we have investigated the effect of specimen size (relative to the cell size) on selected mechanical properties of aluminum foams. Models, described in the companion paper, provide a physical basis for understanding size effects in metallic foams. The models give a good description of size effects in metallic foams.

Keywords: Cellular solids; Size effects; Mechanical properties

1. Introduction

Metallic foams have existed for over 40 years [1]. The development of a number of less costly processing techniques have led to increasing interest in their use in a variety of applications, including lightweight structural sandwich panels and energy absorption devices. The mechanical response of these newer metallic foams, of critical importance in such applications, is currently being evaluated [2–10]. An important issue in mechanical testing of foams is the effect of the specimen size, relative to the cell size, on the measured properties. The size effect is also important in design, as some components may have dimensions of only a few cell diameters (typically, $d \sim 2$–6 mm). In the previous companion paper, we analyzed the effect of the ratio of specimen size to cell size, L/d, on the uniaxial, shear and indentation response of regular, hexagonal honeycombs. The Young's modulus and uniaxial strength were found to increase with increasing values of L/d, up to

* Corresponding author. Tel.: 00-1-617-253-7107; 00-1-617-258-6275.
E-mail address: ljgibson@mit.edu (L.J. Gibson).

0020-7403/01/$ - see front matter
PII: S0020-7403(00)00043-6

a plateau level, corresponding to the bulk properties. The reduced stiffness and strength at lower values of L/d arose from the reduced constraint of cell walls at the free surface as well as from the increasing area fraction of stress-free cell walls. The model for the shear modulus and strength examined the role of a rigid boundary on two parallel faces. The shear moduli and strength decrease with increasing L/d, this time due to the increased constraint of the cell walls at the boundary. The indentation load of a honeycomb is the sum of that required to crush the honeycomb beneath the indenter and that required to yield, and then tear, cell walls at the perimeter of the indenter, allowing it to move through the honeycomb. The indentation strength varies with the inverse of the indenter width. The results for honeycombs were extended to foams by modelling the mechanisms responsible for the size effects.

In this paper, we describe measurements of the effect of specimen size (relative to the cell size) on the mechanical properties (Young's modulus, uniaxial compression strength, shear strength and indentation strength) of aluminum foams. The data are compared with models, derived in the companion paper [14], which provide a physical basis for understanding size effects in metallic foams.

2. Experimental procedure

2.1. Materials

A nominally 7% dense, 20 pore per inch, open-cell aluminum (6101-T6) foam (trade name Duocel; ERG, Oakland, CA) and a nominally 8% dense, closed-cell aluminum foam (trade name Alporas; Shinko Wire, Amagasaki, Japan) were used for the mechanical testing. Their microstructure and mechanical properties have been investigated in a number of studies [3,6–8,11]. The open-cell foam has cells which are elongated in one direction. The cell size was measured using calipers on 6 mm diameter, 12 mm high cylindrical specimens; the small number of cells within the specimens allowed the size of the cells to be measured. The cell size was found to be approximately 4.5 mm parallel to the axis of cell elongation and 3.0 mm in the perpendicular direction. The cell size of the closed cell foam, measured previously using the mean intercept length technique, is 4.5 mm in all three directions [6]. Both foams are transversely isotropic in their mechanical properties. In a given set of tests, the orientation of the specimens remained constant. The open-cell foam was always tested with the loading direction parallel to the axis of cell elongation. The effect of specimen size on the compressive modulus and strength was studied on square prisms of the closed-cell foam and on cylinders of the open-cell material. The effect of specimen size on shear strength and on indentation strength was studied on the closed-cell foam. For each sample in each test the density of the foam was calculated from the measured mass and dimensions of the sample. The density of the closed-cell foam specimens was $223\,kg/m^3$ (with a standard deviation of $8.3\,kg/m^3$) while that of the open-cell foam specimens was $197\,kg/m^3$ (with a standard deviation of $11.6\,kg/m^3$).

2.2. Uniaxial compression tests

The compressive Young's modulus and plastic collapse strength were measured on square prisms of the closed-cell foam with the height, H, equal to twice the cross sectional dimension, L.

The specimen geometry was identical for all the tests but the absolute dimensions were varied such that $L = 8, 12, 17, 24, 30, 36$ and 50 mm. Specimens were cut to the appropriate dimensions using a band saw with a guide to ensure that the cuts were made accurately and straight. Five to nine specimens of each size were tested. The compression tests were carried out on an Instron testing machine (Model 4201, Instron, Canton, MA) with a 5 kN load cell. The software package Labview (National Instruments, Austin, TX) was used to acquire the displacement and load signals from the Instron machine for later processing. The specimens were compressed between steel loading platens. The loading was done in displacement control, at a loading rate such that the imposed strain rate in all the tests was 1×10^{-4}/s. All specimens were loaded to a strain of approximately 20%, well beyond the initial yield strain (of around 2–3%) but before the densification strain (generally 60–70%). During each test the specimen was unloaded just prior to the onset of plastic collapse, then reloaded, and the test continued out to the final strain. This was done to assess the elastic unloading modulus. The compressive stress–strain curves were obtained by dividing the applied load by the original specimen area to obtain the applied stress, and dividing the specimen displacement by the original specimen height to obtain the strain. The specimen displacement was determined by subtracting the displacement corresponding to the testing machine compliance from the measured cross-head displacement. A separate test, with no specimen in place, was done to assess the test machine compliance. It was found that, for the low load levels associated with these foam tests, the displacement associated with the test machine compliance was a small percentage of the total cross-head displacement, no more than 5%.

Localized bands of collapsed cells, giving inhomogeneous deformation and strain, are observed to begin to form in the closed-cell Alporas foam at stresses of about one-half the plateau stress. The strain measured in our tests is the average strain over the entire specimen. The effects of localized plasticity on modulus measurements can be avoided by measuring the unloading modulus; this is the measurement reported here.

Compression tests were also performed on cylinders of the open-cell foam with a height to diameter ratio of two. The cylinder diameter dimensions were: 6.4, 12.7, 19.0, 25.4 and 50.8 mm. Three to five specimens of each size were tested in an Instron testing machine. Displacement was measured using the crosshead displacement as an extensometer could not be attached to the smaller specimens. For comparison, an extensometer was attached to the larger specimens; the moduli measured using the extensometer were about 10% higher than those measured using the crosshead. The crosshead displacement was used in calculating the Young's moduli in all cases. The Young's modulus was taken as the slope of the unloading stress–strain curve at a stress of roughly 0.75 times the compressive plateau stress.

2.3. Shear tests

The shear strength of the closed cell aluminum foam was measured according to ASTM C-273 (Standard Test Method for Shear Properties of Sandwich Core Materials). Five different thicknesses of specimen were tested (6, 12, 18, 24, and 30 mm); the ratio of length to thickness was constant at $l/t = 12$. All of the specimens were of constant width of 50 mm. Five specimens of the 6 mm thick specimens and six specimens of the thicker specimens were tested. The specimens were cut using a band saw and bonded to 12 mm thick milled aluminum plates using a structural adhesive film (FM300, Cytec, Havre de Grace, MD). The adhesive between the specimens and the

plates was cured in an autoclave at a pressure of 0.14 MPa and a temperature of 177°C for 1 h. The shear tests were carried out in an Instron testing machine (Model 1321 , Instron, Canton, MA) with a 50 kN load cell in displacement control such that the imposed strain rate was about 3×10^{-4}/s. Displacement was measured using LVDTs mounted on the plates. Displacement and load signals were acquired using LabView. The shear strength was taken as the peak stress. All specimens were loaded to failure which occurred at a strain of about 2–4%.

2.4. Indentation tests

Axisymmetric indentation tests were carried out on the closed-cell aluminum foam using cylindrical indenters of 6, 12, 24, and 30 mm diameter and between 12 and 20 mm in height. The cylinders were indented up to about 5 mm into a block of foam which was 1.5–3 times the indenter diameter in depth. Each indentation was made at least one indenter diameter away from any other indentations. Preliminary tests showed that this distance was sufficient to avoid edge effects or interference effects between indentations. The indentation tests were performed in an Instron testing machine (Model 1361, Instron, Canton, MA) with a 10 kN load cell at a loading rate of 0.05 mm/s. Displacement was measured from the crosshead displacement and both load and displacement data were acquired using Labview software. At least five indentations were performed for each size of indenter. The indentation stress was calculated from the first peak stress in the load–deflection curve.

3. Results

Typical compressive stress–strain curves for the open- and closed-cell foams, illustrating the unloading response and the initial peak stress, or the plastic collapse stress, are shown in Fig. 1. For the closed-cell foam (Alporas), the slope of the loading curve is less steep than that of the unloading curve, indicating that plastic deformations occur even at stresses well below the plastic collapse strength; this observation is consistent with those of other studies [2,3,6]. Young's modulus is taken as the slope of the unloading curve. The shape of the stress–strain curve is typical of this material, showing an increase up to a peak load, then a drop to a region of more or less constant stress with slight oscillations about the constant stress. For the open-cell foam (Duocel), the stress–strain curve is linear up to the elastic limit. The slope of the initial linear portion of the curve is equal to that of the unloading curve. Beyond the elastic limit the curve is non-linear and reaches a peak stress at a strain of about 1%, after which the stress remains roughly constant. For each material, the shape of the curve was similar for the entire range of specimen sizes, although the actual values of stiffness and strength varied for the different specimen sizes.

The average density, Young's modulus and compressive strength for each size of specimen tested are listed in Table 1. The Young's modulus and peak stress, normalized by those of the bulk material, are plotted against the specimen size, L, relative to the cell size, d, in Figs. 2 and 3. The modulus increases with increasing normalized specimen size up to a plateau level at $L/d \approx 6$ for both foams. The modulus of the bulk material was taken as the average value for $L/d > 6$ ($E_{\text{bulk}} = 943$ MPa for Alporas and $E_{\text{bulk}} = 368$ MPa for Duocel). For $L/d < 6$, the Young's modulus of the open-cell foam drops more rapidly with decreasing L/d than that for the closed-cell

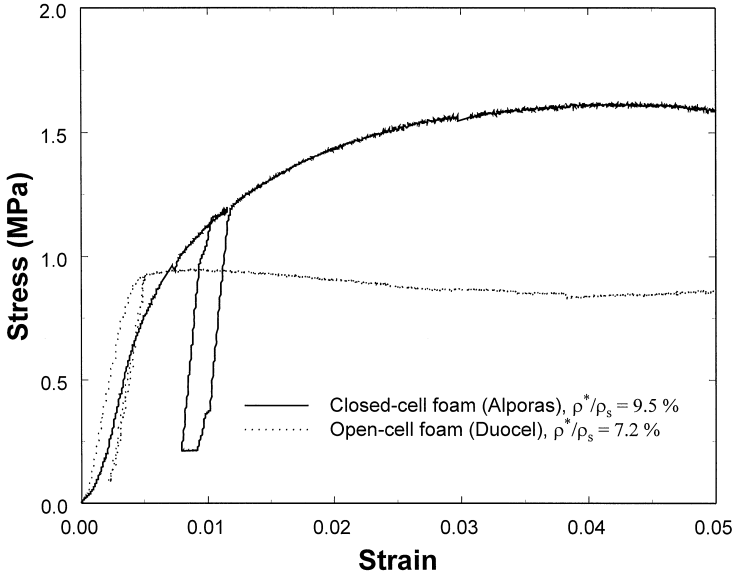

Fig. 1. Typical compressive stress–strain curves for closed cell (Alporas) and open cell (Duocel) aluminum foam.

Table 1
Uniaxial compression data for specimens of varying size

L (mm)	Density (g/mm^3)	E_{unload} (MPa)	σ^*_{pl} (MPa)
Alporas foam results			
Square prisms $L \times L \times 2L$			
50	0.2175 (0.0018)	943 (27)	1.51 (0.02)
36	0.2169 (0.0018)	913 (24)	1.44 (0.05)
30	0.2276 (0.0016)	910 (39)	1.48 (0.04)
24	0.2290 (0.0016)	792 (39)	1.47 (0.05)
17	0.2282 (0.0041)	612 (69)	1.18 (0.11)
12	0.2169 (0.0054)	652 (76)	1.07 (0.06)
8	0.2277 (0.0166)	384 (58)	0.95 (0.19)
Duocel foam results			
Specimens: Cylinders, $H = 2D$			
D (mm)	Density (g/mm^3)	E_{unload} (MPa)	σ^*_{pl} (MPa)
50.8	0.1863 (0.0027)	357 (6)	1.35 (0.07)
25.4	0.1877 (0.0046)	379 (39)	1.37 (0.25)
19.05	0.2003 (0.0086)	369 (90)	1.19 (0.42)
12.7	0.2014 (0.0095)	287 (61)	1.00 (0.06)
6.35	0.2052 (0.0159)	118 (52)	0.56 (0.27)

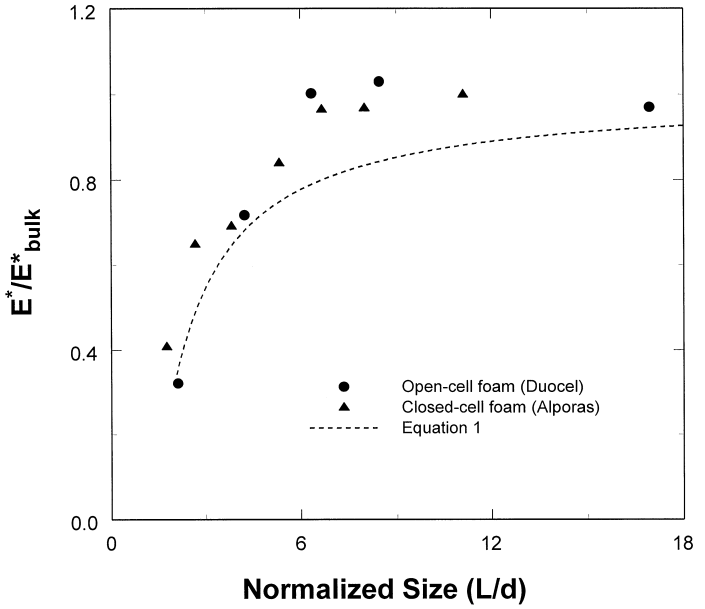

Fig. 2. Unloading Young's modulus, normalized by the bulk value, plotted against specimen edge length, L, normalized by the cell size, d, for the open- and closed-cell aluminum foams.

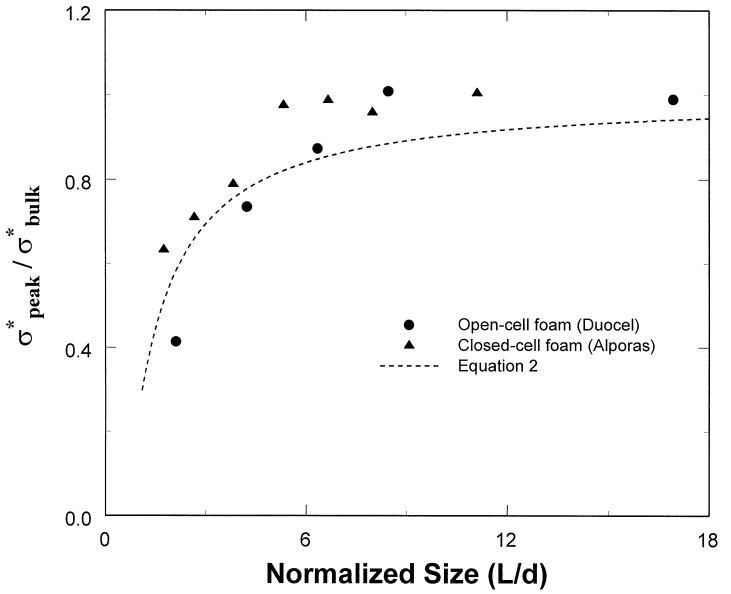

Fig. 3. Plastic collapse strength, normalized by the bulk value, plotted against specimen diameter, L, normalized by the cell size, d, for the open- and closed-cell aluminum foams.

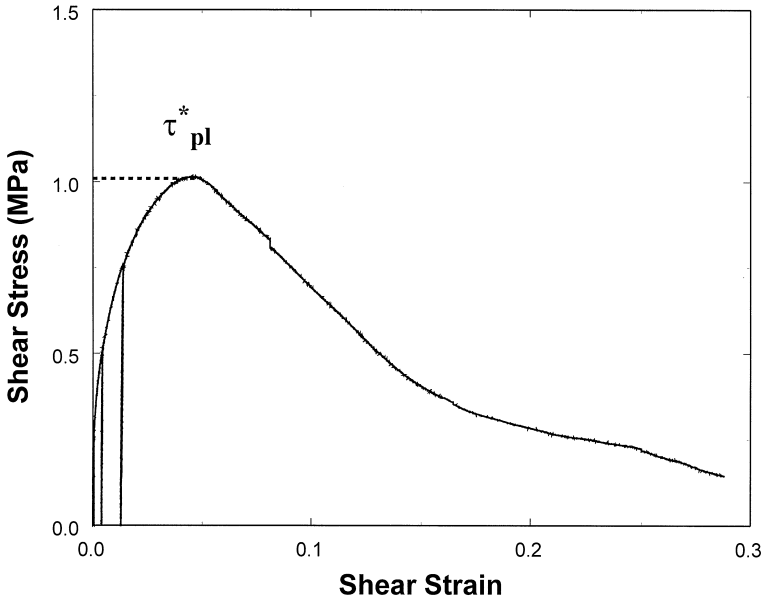

Fig. 4. Typical shear stress–shear strain curve for the closed-cell aluminum foam (Alporas) ($t = 30$ mm).

foam. The normalized peak stress follows a similar pattern, increasing with L/d up to a plateau level at $L/d = 8$ for the open-cell foam and at $L/d = 5$ for the closed-cell foam. At lower values of L/d, the peak stress of the open-cell foam falls more rapidly with decreasing L/d than that for the closed cell foam. The peak stress of the bulk material was taken as the average value for $L/d > 8$ or 5 for the open- and closed-cell foams, respectively ($\sigma^*_{pl} = 1.35$ MPa for Duocel and $\sigma^*_{pl} = 1.51$ MPa for Alporas). The bulk values for both the Young's modulus and the peak stress are comparable to those measured by Simone and Gibson [6] on 50 mm × 50 mm × 100 mm prisms.

A typical shear stress–strain curve for the closed-cell foam (Alporas) is shown in Fig. 4. The shear strength, normalized by the bulk value, is plotted against the ratio of specimen thickness, t, to cell size, d, in Fig. 5. The average density of the 12, 18, 24 and 30 mm specimens was 212 kg/m^3 with a standard deviation of about 8 kg/m^3. The densities of the five 6 mm thick specimens were significantly lower: 180, 182, 183, 189 and 210 kg/m^3. The average shear strength of the three lower density 6 mm thick specimens was 1.11 MPa, compared with 1.36 MPa for the 189 kg/m^3 and 1.64 MPa for the 210 kg/m^3 density specimens. Density variations between specimens of different thicknesses were minimized by reporting, for each thickness over 6 mm, the average shear strength of the three specimens with densities closest to 200 kg/m^3. The individual data points for the 189 and 210 kg/m^3 densities of the 6 mm specimens are plotted on Fig. 5: their average shear strength is 1.50 MPa. The shear strength of the thicker specimens is roughly constant at a value of 1.02 MPa. The shear strength becomes independent of the specimen thickness at $t/d = 2.67$.

A typical stress–displacement curve for an indentation test is shown in Fig. 6. The indentation stress, reached at a displacement of about 1mm, is roughly constant. The indentation stress,

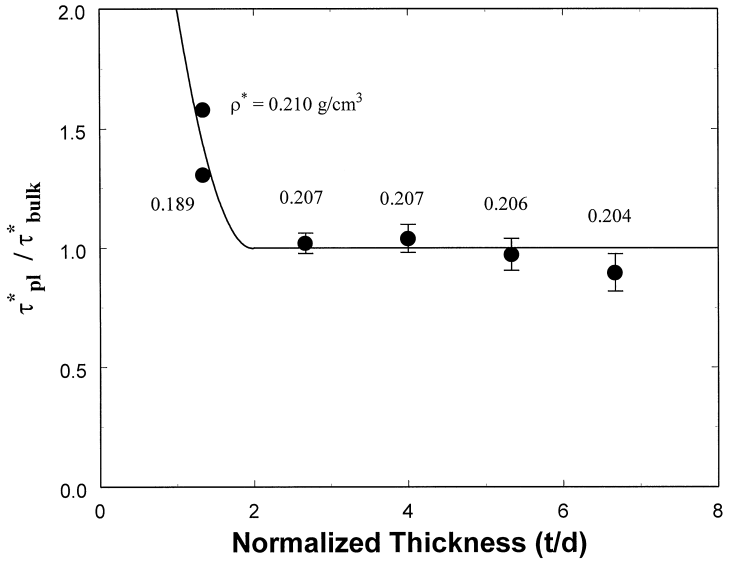

Fig. 5. Shear strength, normalized by the bulk value, plotted against the ratio of specimen thickness, t, to the cell size, d, for the closed-cell foam (Alporas).

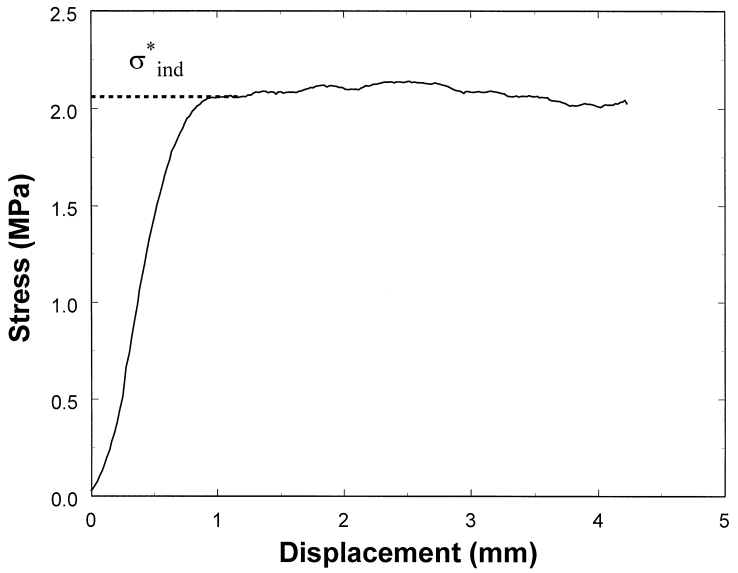

Fig. 6. Indentation stress–displacement curve for the closed-cell foam (Alporas) for an indenter diameter of 30 mm.

normalized by the plastic collapse strength, is plotted against the ratio of indenter diameter, D, to cell size, d, in Fig. 7: it increases as the inverse of the indenter diameter. The value of the indentation stress for large indenter diameters approaches a value slightly higher than the uniaxial compressive strength of the material (1.42 MPa).

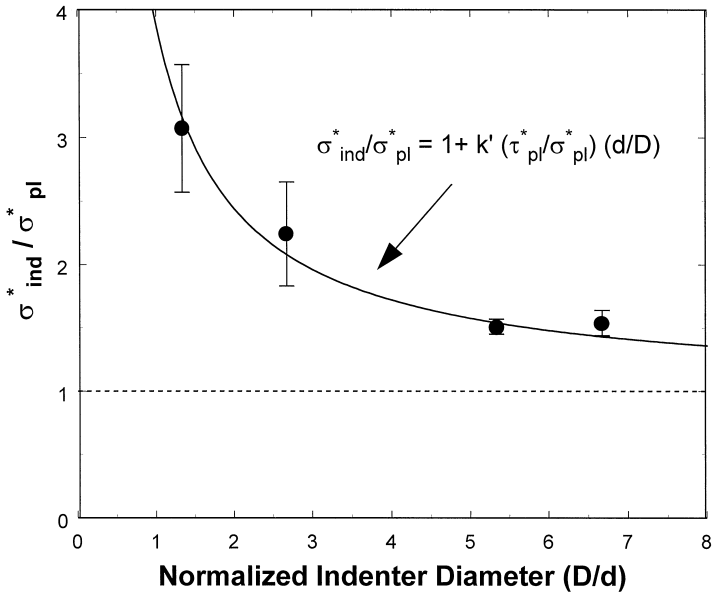

Fig. 7. Indentation peak stress, normalized by the plastic collapse strength, plotted against the ratio of indenter diameter, D, to cell size, d, for the closed-cell aluminum foam (Alporas). The solid line represents Eq. (3).

4. Discussion

4.1. Uniaxial compression

The effect of the ratio of specimen size to cell size on the Young's modulus of a honeycomb was analyzed in the previous companion paper by considering two contributions: the decreased constraint at the free surface of the foam, giving a less stiff boundary layer, and the area fraction of cut cell walls at the boundary which remain stress-free. For a foam, both effects give (Eq. (35) of the previous, companion paper) [14]

$$\frac{E}{E_{\text{bulk}}} = \left(1 - 2n\frac{d}{L} - 2p\frac{d}{L}\right)^2 + 4nm\left(\frac{d}{L}\right)\left[1 - 2n\frac{d}{L} - 2p\frac{d}{L}\right] + 4n^2m^2\left(\frac{d}{L}\right)^2, \tag{1}$$

where m is the reduced stiffness factor for the boundary layer of thickness nd and the stress free layer of zero stiffness is of thickness pd. Eq. (1) is plotted on Fig. 2 with $m = 0.85$, $n = 0.5$ and $p = 0.25$; it follows the general trend of the data but reaches the plateau value for the modulus at higher values of L/d.

The normalized moduli for the open-cell foam decrease more rapidly with decreasing L/d than those for the closed-cell foam. Two factors contribute to this. The cell faces in the closed-cell foam may increase the stiffness of its boundary layer compared with that for the open-cell foam. And the cut cell edges of the open-cell foam are stress-free, like those of the honeycomb, while the cut cell edges and faces at the boundary of the closed cell foam are not completely stress-free, due to the presence of the faces.

The size effect for the uniaxial compressive strength of a honeycomb arises from the stress-free walls at the boundary of the honeycomb. Analysis of the same phenomenon in foams gives [14]

$$\frac{\sigma_{\mathrm{pl}}}{\sigma^*_{\mathrm{pl}}} = \frac{(L/d - 1/2)^2}{(L/d)^2}. \tag{2}$$

Eq. (2) is plotted along with the data shown in Fig. 3; it describes the data well. We note that the normalized strength decreases more rapidly with decreasing L/d for the open-cell than the closed-cell foam, again, due to the effect of the cell faces.

Both our data and models suggest that the bulk values of both Young's modulus and strength are reached at values of L/d of about 5–8, lower than the value of 15 suggested by Brezny and Green [12]. The discrepancy may be due to a difference in test methods. They used three point bend specimens which subject the more compliant top and bottom surfaces of the beam to the highest normal stresses, magnifying the size effect in smaller beams and increasing the critical value of L/d. Their tests were performed on a brittle reticulated vitreous carbon foam which exhibits a Weibull size effect, confounding the specimen size/cell size effect.

The trends we observe in stiffness and strength are similar to those of Bastawros et al. [13]. In that study, uniaxial compression tests were performed on prismatic aluminum foam specimens of constant length and width and varying depth. They found that stiffness and strength became essentially constant when the depth was greater than about 4 times the cell size.

4.2. Shear strength

The normalized shear strength of the closed-cell foam decays rapidly to a plateau value at a ratio of the specimen thickness to cell size, t/d, of 2. Since there are no stress or strain gradients in the out-of-plane direction in the shear test, the two-dimensional honeycomb analysis of size effects on shear strength can be applied directly to foams. Assuming that, on average, the cell edges and faces are cut at the midpoint along their length, the honeycomb analysis indicates that $\tau^*_{\mathrm{pl}}/\tau^*_{\mathrm{bulk}} = 2$ for $t/d = 1$, and that $\tau^*_{\mathrm{pl}}/\tau^*_{\mathrm{bulk}}$ decays to a value of unity for $t/d \geqslant 2$ [14], in close agreement with our experimental results (Fig. 5).

4.3. Indentation

The indentation stress varies with the inverse of the indenter diameter, D. In an indentation test, the foam immediately below the indenter crushes and the foam at the perimeter of the indentation yields in shear and then ruptures (Fig. 8). The total force on the indenter is the sum of the crushing force (equal to the plastic collapse strength of the foam times the cross sectional area) and the shearing force (equal to the shear strength of the foam times the perimeter)

$$P_{\mathrm{ind}} = P_{\mathrm{crush}} + P_{\mathrm{shear}} = \sigma^*_{\mathrm{pl}} \frac{\pi D^2}{4} + k\tau^*_{\mathrm{pl}} \pi D d$$

or

$$\frac{\sigma^*_{\mathrm{ind}}}{\sigma^*_{\mathrm{pl}}} = 1 + k' \left(\frac{\tau^*_{\mathrm{pl}}}{\sigma^*_{\mathrm{pl}}}\right) \frac{d}{D}. \tag{3}$$

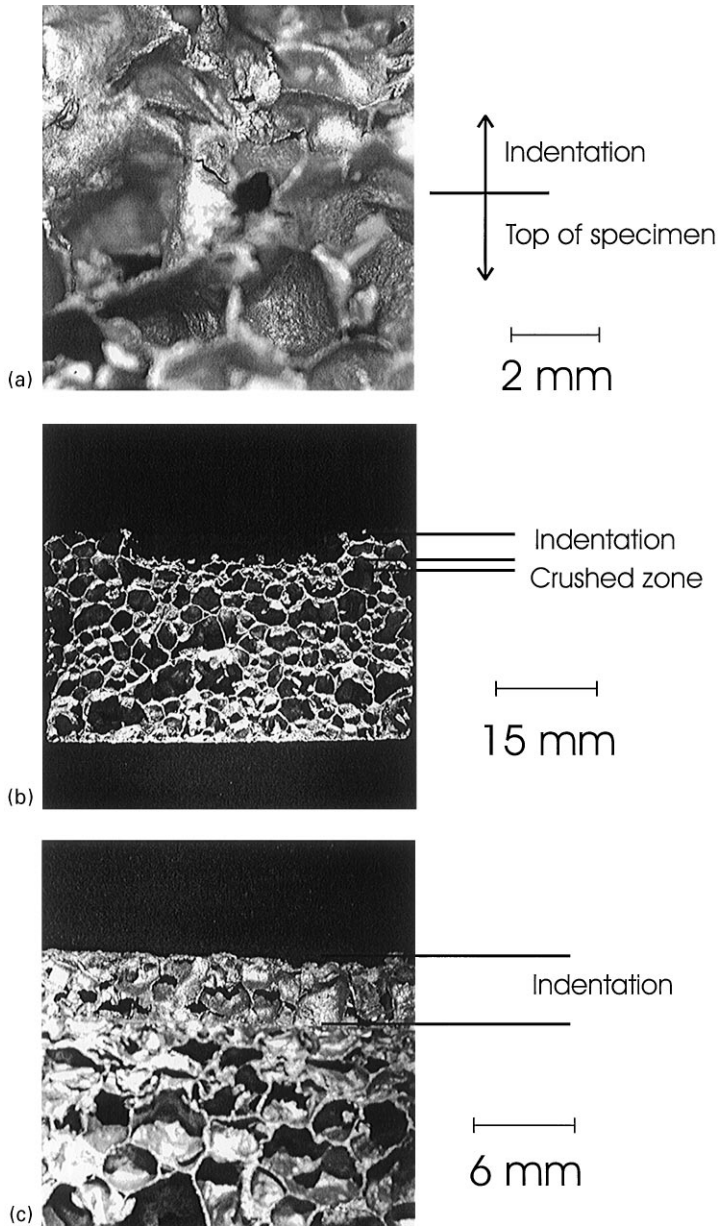

Fig. 8. Optical photographs of indentation specimens. (a) Specimen loaded to the initial peak stress and then unloaded. View from above the indentation showing torn cell walls at perimeter of indentation. (b, c) Longitudinal section of a specimen loaded beyond the initial peak stress and then unloaded, showing the indentation, the crushed zone beneath the indentation and torn cell walls on the back wall of the perimeter of the indentation.

Eq. (3) is compared with the indentation data in Fig. 7 using our measured values for $\sigma^*_{\rm pl} = 1.42$ MPa and $\tau^*_{\rm pl} = 1.03$ MPa. We find a value of $k' = 3.98$ from the fit of Eq. (3) to the data, giving $k = 1$. This suggests that yielding at the boundary of the indenter extends to a depth of about 1 cell into the foam. The indentation data are well described by Eq. (3).

5. Conclusions

The Young's modulus and plastic collapse strength of both the closed-cell Alporas and the open-cell Duocel foams increased to a plateau level as the ratio of specimen size to cell size increased. The plateau values were reached at $L/d = 6$ for the Young's modulus for both foams and at $L/d = 8$ and 5 for the compressive strength of the open- and closed-cell foams, respectively. The modulus and strength of the open-cell foam decreased more rapidly with decreasing L/d than those of the closed-cell foam due to the effect of the cell faces. Extrapolation of the analytical models for size effects in honeycombs to foams gives a good description of the data for uniaxial loading.

The size effect for the shear strength vanishes for specimens with a thickness of at least twice the cell size. The two-dimensional honeycomb model for the effect of t/d on the shear strength (which is also applicable to foams) describes the data for the closed-cell aluminum foam well.

The indentation strength decreases as the size of the indenter increases relative to the cell size and approaches a limiting value slightly higher than the uniaxial plastic collapse strength of the foam. The decrease varies as the inverse of the indenter diameter. This can be understood in terms of the observation that during an indentation test the foam immediately below the indenter crushes and the cell walls at the perimeter of the indentation yield and then rupture. A simple model gives a good description of the data.

Acknowledgements

We are grateful for financial support of ARPA (Contract number N00014-96-1-1028). Some of the tests on the effect of specimen size on the compressive modulus and strength of the open-cell foam were performed by Dr. A.E. Simone, whose assistance is appreciated. The research of Dr. P. Onck has been made possible by a fellowship of the Royal Netherlands Academy of Arts and Sciences. The assistance of Prof. J.W. Hutchinson is highly appreciated. Figs. 2, 4 and 5 appear with permission, from the Annual Review of Material Science, volume 30 copyright 2000 by Annual Reviews www.AnnualReviews.org.

References

[1] Elliot JC. Method of producing metal foam. U.S. Patent No 2,751,289, 1956.
[2] Gradinger R, Simancik F, Degischer HP. Determination of mechanical properties of foamed metals. International Conference Welding Technology, Materials and Materials Testing, Fracture Mechanics and Quality Management, Vienna University of Technology, 1997.
[3] Sugimura Y, Meyer J, He MY, Bart-Smith H, Grenestedt J, Evans AG. On the mechanical performance of closed cell foams. Acta Materiala 1997;45:5245–59.
[4] Bart-Smith H, Bastawros A-F, Mumm DR, Evans AG, Sypeck DJ, Wadley HNG. Compressive deformation and yielding mechanisms in cellular Al alloys determined using X-ray tomography and surface strain mapping. Acta Materiala 1998;46:3583–92.
[5] Evans AG, Hutchinson JW, Ashby MF. Multifunctionality of cellular metal systems. Progress in Materials Science 1998;43:171–221.
[6] Simone AE, Gibson LJ. Aluminum foams produced by liquid state processes. Acta Materiala 1998;46:3109–23.

[7] von Hagen H, Bleck W. Compressive, tensile and shear testing of melt-foamed aluminum. Symposium R: Porous and Cellular Materials for Structural Applications, Materials Research Society Spring Meeting 1998, San Francisco.
[8] Andrews EW, Sanders W, Gibson LJ. Compressive and tensile behaviour of aluminum foams. Materials Science and Engineering A 1999;270:113–24.
[9] Deshpande, Fleck NA. Isotropic constitutive models for metallic foams. Journal of the Mechanics and Physics of Solids 2000;48:1253–83.
[10] Harte A-M, Fleck NA, Ashby MF. Fatigue failure of an open cell and a closed cell aluminum alloy foam. Acta Materiala 1999;47:2511–24.
[11] Gioux G, McCormack TM, Gibson LJ. Failure of aluminum foams under multiaxial loads. International Journal of Mechanical Sciences 2000;42:1097–117.
[12] Brezny R, Green DJ. Characterization of edge effects in cellular materials. Journal of Materials Science 1990;25:4571–8.
[13] Bastawros A-F, Bart-Smith H, Evans AG. Experimental analysis of deformation mechanisms in a closed-cell Al alloy foam. Journal of the Mechanics and Physics of Solids 2000;48:301–22.
[14] Onck PR, Andrews EW, Gibson LJ. Size effects in ductile cellular solids Part I: Modelling. International Journal of Mechanical Sciences 2001;43:681–99.